

Preparation, Characterization, and Photophysical Properties of *cis*- or *trans*-PtLn₂ (Ln = Nd, Eu, Yb) Arrays with 5-Ethynyl-2,2'-bipyridine

Hai-Bing Xu,[†] Jun Ni,[†] Kun-Jiao Chen,[†] Li-Yi Zhang,[†] and Zhong-Ning Chen^{*,†,‡}

State Key Laboratory of Structural Chemistry, Fujian Institute of Research on the Structure of Matter, Chinese Academy of Sciences, Fuzhou, Fujian 350002, People's Republic of China, and State Key Laboratory of Organometallic Chemistry, Shanghai Institute of Organic Chemistry, Chinese Academy of Sciences, Shanghai 200032, People's Republic of China

Received June 25, 2008

Reaction of *cis*- or *trans*-Pt(PPh₃)₂Cl₂ (PPh₃ = triphenylphosphine) with 5-[2-(trimethylsilyl)-1-ethynyl]-2,2'-bipyridine (bpyC≡CSiMe₃) gave *cis*-Pt(PPh₃)₂(C≡Cbpy)₂ (**1**) or *trans*-Pt(PPh₃)₂(C≡Cbpy)₂ (**5**). Incorporating **1** or **5** with Ln(hfac)₃(H₂O)₂ (hfac = hexafluoroacetylacetonate) induced formation of the corresponding *cis*- or *trans*-PtLn₂ heterotrimeric complexes *cis*-Pt(PPh₃)₂{(C≡Cbpy)Ln(hfac)₃}₂ (Ln = Nd **2**, Eu **3**, Yb **4**) or geometrical isomers *trans*-Pt(PPh₃)₂{(C≡Cbpy)Ln(hfac)₃}₂ (Ln = Nd **6**, Eu **7**, Yb **8**). As verified through ³¹P NMR characterization as well as determination of the structures of **1**, **4**, and **8** by X-ray crystallography, the *cis*- or *trans*-arranged forms around Pt^{II} centers remain unchanged in both solutions and solid states without thermal or light-induced isomerization during the reactions. With excitation at 360 < λ_{ex} < 450 nm, which is the absorption region of metal-perturbed π→π* (C≡C) transitions and dπ(Pt)→π*(C≡Cbpy) MLCT transition, sensitized lanthanide luminescence occurs with a microsecond range of lifetimes in both *cis*- and *trans*-arranged PtLn₂ complexes, revealing that efficient Pt→Ln energy transfer is indeed operating from the platinum(II) acetylide chromophore to lanthanide centers.

Introduction

The chemistry of heterometallic and/or multicomponent alkynyl complexes has recently received more and more attention in view of their extensive applications as nonlinear optical materials, organic light emitting diodes (OLED), luminescence sensors, molecular devices, etc.^{1–5} Among various classes of organic ligands, polypyridyl-functionalized alkynyl ligands are particularly useful for the design of heterometallic and/or multicomponent arrays as optoelectronic materials at the molecular level.^{6,7} Their bifunctional character makes them favorable bridging ligands capable of connecting with two types of organometallic chromophores or emitters through both metal–alkynyl coordination and metal–polypyridyl chelation.^{8–16} The “soft” ethynyl C donors are usually σ-bonded to d-block

metal ions, whereas the “hard” polypyridyl N donors are frequently chelated to lanthanide centers. This affords a feasible approach for the design of d–f heterometallic arrays containing both transition metal and lanthanide ions,^{17–23} where effective energy transfer usually occurs from d-block organometallic chromophores to lanthanide centers, thus inducing sensitized lanthanide luminescence by excitation of d-block organometallic chromophores in the near-UV–vis region. As a typical bifunctional alkynyl ligand, 5-ethynyl-2,2'-bipyridine is feasible for the design of heterometallic and/or multicomponent arrays containing a prefabricated platinum(II) bis(σ-acetylide) module with square-planar geometry, in which subsequently introducing d-block metal or lanthanide subunits through 2,2'-chelation

* To whom correspondence should be addressed. E-mail: czn@fjirsm.ac.cn.

[†] Fujian Institute of Research on the Structure of Matter.

[‡] Shanghai Institute of Organic Chemistry.

(1) Lang, H.; Packheiser, R. *Collect. Czech. Chem. Commun.* **2007**, *72*, 435.

(2) Ren, T. *Organometallics*. **2005**, *24*, 4854.

(3) Wong, K. M.-C.; Hui, C.-K.; Yu, K.-L.; Yam, V. W.-W. *Coord. Chem. Rev.* **2002**, *229*, 123.

(4) Abu-Salah, O. M. J. *Organomet. Chem.* **1998**, *565*, 211.

(5) Chen, Z.-N.; Zhao, N.; Fan, Y.; Ni, J. *Coord. Chem. Rev.* **2008**, DOI: 10.1016/j.ccr.2007.11.015.

(6) Ziessel, R.; Hissler, M.; El-ghayoury, A.; Harriman, A. *Coord. Chem. Rev.* **1998**, *178–180*, 1251.

(7) Chen, Z.-N.; Fan, Y.; Ni, J. *Dalton Trans* **2008**, 573.

(8) Wei, Q.-H.; Yin, G.-Q.; Zhang, L.-Y.; Chen, Z.-N. *Inorg. Chem.* **2006**, *45*, 10371.

(9) Xu, H.-B.; Zhang, L.-Y.; Chen, Z.-N. *Inorg. Chim. Acta* **2007**, *360*, 163.

(10) Fan, Y.; Zhang, L.-Y.; Dai, F.-R.; Shi, L.-X.; Zhao, N.; Chen, Z.-N. *Inorg. Chem.* **2008**, *47*, 2811.

(11) Schmittel, M.; Kalsani, V.; Bats, J. W. *Inorg. Chem.* **2005**, *44*, 4115.

(12) Pomestchenko, I. E.; Polyansky, D. E.; Castellano, F. N. *Inorg. Chem.* **2005**, *44*, 3412.

(13) Shiotsuka, M.; Yamamoto, Y.; Okuno, S.; Kitou, M.; Nozaki, K.; Onaka, S. *Chem. Commun.* **2002**, 590.

(14) Harriman, A.; Hissler, M.; Ziessel, R.; De Cian, A.; Fisher, J. J. *Chem. Soc., Dalton Trans.* **1995**, 4067.

(15) Hissler, M.; Ziessel, R. *J. Chem. Soc., Dalton Trans.* **1995**, 893.

(16) Ziessel, R.; Diring, S.; Retailleau, P. *Dalton Trans.* **2006**, 3285.

(17) Ward, M. D. *Coord. Chem. Rev.* **2007**, *251*, 1663.

(18) Xu, H.-B.; Shi, L.-X.; Ma, E.; Zhang, L.-Y.; Wei, Q.-H.; Chen, Z.-N. *Chem. Commun.* **2006**, 1601.

(19) Ronson, T. K.; Lazarides, T.; Adams, H.; Pope, S. J. A.; Sykes, D.; Faulkner, S.; Coles, S. J.; Hursthouse, M. B.; Clegg, W.; Harrington, R. W.; Ward, M. D. *Chem.–Eur. J.* **2006**, *12*, 9299.

(20) Ziessel, R.; Diring, S.; Kadjane, P.; Charbonnière, L.; Retailleau, P.; Philouze, C. *Chem. Asian J.* **2007**, *2*, 975.

(21) Xu, H.-B.; Zhang, L.-Y.; Xie, Z.-L.; Ma, E.; Chen, Z.-N. *Chem. Commun.* **2007**, 2744.

(22) Li, X.-L.; Shi, L.-X.; Zhang, L.-Y.; Wen, H.-M.; Chen, Z.-N. *Inorg. Chem.* **2007**, *46*, 10892.

(23) Li, X.-L.; Dai, F.-R.; Zhang, L.-Y.; Zhu, Y.-M.; Peng, Q.; Chen, Z.-N. *Organometallics* **2007**, *26*, 4483.

provides an excellent approach to access a series of multicomponent complexes with desired spatial orientations.^{7–9,18,21}

Platinum(II) acetylide complexes have been extensively investigated owing to their multifold applications in various optical materials,^{6,7,24} single-molecule insulators,^{25,26} molecular electronics, etc.²⁷ The platinum(II) centers usually exhibit square-planar geometry with bis(σ -acetylide) oriented in *cis* or *trans* form. Taking judicious advantage of a prefabricated *cis* or *trans* arrangement, stereochemical structures can be elaborately envisaged.^{28–34} These *cis*- or *trans*-platinum(II) bis(σ -acetylide) species are kinetically stable in solutions without thermal or light-induced isomerization, thus facilitating exact positioning prefabricated modules into ordered arrays.^{14,15,28} A series of Pt–Ln heteronuclear species with polypyridyl alkynyl ligands have been prepared in our laboratory using *cis*- or *trans*-arranged square-planar platinum(II) bis(acetylide) complexes as precursors to incorporate Ln(hfac)₃ units,^{21–23} in which sensitized lanthanide(III) luminescence is successfully achieved by effective Pt→Ln energy transfer from a platinum(II) bis(acetylide) antenna chromophore. Since the photons collected by the central platinum(II) site can be quantitatively transferred to the peripheral lanthanide(III) emitters, the central platinum(II) bis(σ -acetylide) chromophore serves as an efficient near-UV light harvesting antenna. In order to explore the influence of geometric orientations in the central platinum(II) bis-acetylide antenna chromophore on Pt→Ln energy transfer and subsequently sensitized lanthanide(III) luminescence in Pt–Ln complexes, we are interested in the construction of a series of *cis*- and *trans*-PtLn₂ heterotrimeric isomers with 5-ethynyl-2,2'-bipyridine. We describe herein the use of *cis*- and *trans*-platinum(II) bis- σ -acetylide isomers as prefabricated modules for the preparation of a series of *cis*- and *trans*-PtLn₂ heterotrimeric isomeric complexes by incorporating Ln(hfac)₃ (Ln = Nd, Eu, Yb; hfac = hexafluoroacetylacetonate) units through 2,2'-bipyridyl chelation. For both *cis*- and *trans*-PtLn₂ isomers, sensitized lanthanide luminescence is indeed achieved with excitation at 360 nm < λ_{ex} < 450 nm, which is the absorption region of platinum(II) bis-acetylide chromophores, revealing unambiguously that substantial Pt→Ln energy transfer occurs from Pt-based organometallic antenna chromophores in these *cis*- and *trans*-PtLn₂ arrays.

(24) Zhou, G.-J.; Wong, W.-Y.; Lin, Z.; Ye, C. *Angew. Chem., Int. Ed.* **2006**, *45*, 6189.

(25) Mayor, M.; Hänisch, C. V.; Weber, H. B.; Reichert, J.; Beckmann, D. *Angew. Chem., Int. Ed.* **2002**, *41*, 1183.

(26) Schull, T. L.; Kushmerick, J. G.; Patterson, C. H.; George, C.; Moore, M. H.; Pollack, S. K.; Shashidhar, R. *J. Am. Chem. Soc.* **2003**, *125*, 3202.

(27) Silverman, E. E.; Cardolaccia, T.; Zhao, X. M.; Kim, K. Y.; Haskins-Glusac, K.; Schanze, K. S. *Coord. Chem. Rev.* **2005**, *249*, 1491.

(28) Johnson, C. A.; Haley, M. M.; Rather, E.; Han, F.; Weakley, T. J. R. *Organometallics* **2005**, *24*, 1161.

(29) DʼAmato, R.; Furlani, A.; Colapietro, M.; Portalone, G.; Casalboni, M.; Falconieri, M.; Russo, M. V. *J. Organomet. Chem.* **2001**, *627*, 13.

(30) Campbell, K.; McDonald, R.; Ferguson, M. J.; Tykwinski, R. R. *J. Organomet. Chem.* **2003**, *683*, 397.

(31) Jude, H.; Disteldorf, H.; Fischer, S.; Wedge, T.; Hawkrige, A. M.; Arif, A. M.; Hawthorne, M. F.; Muddiman, D. C.; Stang, P. J. *J. Am. Chem. Soc.* **2005**, *127*, 12131.

(32) Peters, T. B.; Zheng, Q.; Stahl, J.; Bohling, J. C.; Arif, A. M.; Hampel, F.; Gladysz, J. A. *J. Organomet. Chem.* **2002**, *641*, 53.

(33) Tao, C. H.; Wong, K. M.-C.; Zhu, N. Y.; Yam, V. W.-W. *New J. Chem.* **2003**, *27*, 150.

(34) Onitsuka, K.; Fujimoto, M.; Ohshiro, N.; Takahashi, S. *Angew. Chem., Int. Ed.* **1999**, *38*, 689.

Experimental Section

General Procedures. All manipulations were performed under a dry argon atmosphere using Schlenk techniques and a vacuum-line system. The solvents were dried, distilled, and degassed prior to use except that those for spectroscopic measurements were of spectroscopic grade. The reagents potassium tetrachloroplatinum (K₂[PtCl₄]), 2,2'-bipyridine (bpy), triphenylphosphine (PPh₃), and hexafluoroacetylacetonate (hfac) were commercially available. 5-[2-(Trimethylsilyl)-1-ethynyl]-2,2'-bipyridine (bpyC≡CSiMe₃),³⁵ *trans*-Pt(PPh₃)₂Cl₂,³⁶ and *cis*-Pt(PPh₃)₂Cl₂³⁷ were prepared by literature procedures.

Ln(hfac)₃(H₂O)₂ (Ln = Nd, Eu, Yb) were prepared by modification of the literature procedures³⁸ as follows. To an aqueous solution of lanthanide(III) acetate (pH = 5–7) was added dropwise 3.3 equiv of hfac with stirring at room temperature for 3 h. The precipitate was filtered, washed with water, and dried under vacuum to afford the quantitative product.

***cis*-Pt(PPh₃)₂(C≡Cbpy)₂ (1).** To a THF (30 mL) solution of bpyC≡CSiMe₃ (160 mg, 0.64 mmol) and *cis*-PtCl₂(PPh₃)₂ (221 mg, 0.28 mmol) were added a solution of CuI (5 mg) in acetonitrile (2 mL) and a methanol (5 mL) solution of KF (58 mg, 1.0 mmol) with stirring at room temperature for five days. The solution was concentrated by rotary evaporation to give the crude product, which was purified by silica gel column chromatography. Elution with dichloromethane–methanol (v/v = 100:2) gave a pale yellow product. Yield: 66% (200 mg). Anal. Calcd for C₆₀H₄₄N₄P₂Pt: C, 66.85; H, 4.11; N, 5.20. Found: C, 66.43; H, 4.18; N, 5.34. ESI-MS (CH₃OH–CH₂Cl₂): *m/z* (%) 1079 (100) ([M + H]⁺), 816 (5) ([M – PPh₃ + H]⁺). IR (KBr, cm⁻¹): 2115s (C≡C). ¹H NMR (CDCl₃, ppm): 8.61 (s, 2H, bpyC≡C), 8.22 (d, 2H, *J* = 7.92 Hz, bpyC≡C) 7.93 (d, 2H, *J* = 8.25 Hz, bpyC≡C), 7.81 (d, 14H, *J* = 5.58 Hz, C₆H₅ and bpyC≡C), 7.72 (d, 2H, *J* = 7.8 Hz, bpyC≡C), 7.65 (s, 2H, bpyC≡C), 7.4 (d, 18H, *J* = 7.56 Hz, C₆H₅ and bpyC≡C), 6.61 (d, 2H, *J* = 8.25 Hz, bpyC≡C). ³¹P NMR (CDCl₃, ppm): 21.5 (t, *J*_{Pt–P} = 2648 Hz).

***cis*-Pt(PPh₃)₂{(C≡Cbpy)Ln(hfac)₃}₂ (Ln = Nd, Eu, Yb).** These PtLn₂ complexes were prepared by addition of 2.2 equiv of Ln(hfac)₃(H₂O)₂ to a dichloromethane solution of **1** with stirring for 1 h. After filtering, the concentrated dichloromethane solutions were layered with hexane to afford the products as pale yellow crystals. Yield: 68–75%.

2 (Ln = Nd). Anal. Calcd for C₉₀H₅₀Nd₂F₃₆N₄O₁₂P₂Pt: C, 41.44; H, 1.93; N, 2.15. Found: C, 41.54; H, 2.05; N, 2.21. IR (KBr, cm⁻¹): 2120m (C≡C), 1651s (C=O).

3 (Ln = Eu). Anal. Calcd for C₉₀H₅₀Eu₂F₃₆N₄O₁₂P₂Pt: C, 41.19; H, 1.92; N, 2.13. Found: C, 41.44; H, 1.85; N, 2.11. IR (KBr, cm⁻¹): 2120m (C≡C), 1651s (C=O).

4 (Ln = Yb). Anal. Calcd for C₉₀H₅₀F₃₆N₄O₁₂P₂PtYb₂: C, 40.54; H, 1.89; N, 2.10. Found: C, 40.94; H, 1.87; N, 2.01. IR (KBr, cm⁻¹): 2120m (C≡C), 1651s (C=O).

***trans*-Pt(PPh₃)₂(C≡Cbpy)₂ (5).** This compound was prepared by the same procedure as that of **1** except using *trans*-Pt(PPh₃)₂Cl₂ instead of *cis*-Pt(PPh₃)₂Cl₂. The product was purified by silica gel column chromatography using dichloromethane as an eluent. Recrystallization of the product by slow diffusion of hexane into a dichloromethane solution afforded **5** as pale yellow crystals. Yield: 79%. Anal. Calcd for C₆₀H₄₄N₄P₂Pt: C, 66.85; H, 4.11; N, 5.20. Found: C, 66.63; H, 4.08; N, 5.14. ESI-MS (CH₃OH–CH₂Cl₂):

(35) (a) Grossshenny, V.; Romero, F. M.; Ziessel, R. *J. Org. Chem.* **1997**, *62*, 1491. (b) Ziessel, R.; Suffert, J.; Youinou, M.-T. *J. Org. Chem.* **1996**, *61*, 6535.

(36) Hsu, C.-Y.; Leshner, B. T.; Orchin, M. *Inorg. Synth.* **1979**, *19*, 114.

(37) Jensen, K. A. Z. *Anorg. Allg. Chem.* **1936**, *229*, 265.

(38) Hasegawa, Y.; Kimura, Y.; Murakoshi, K.; Wada, Y.; Kim, J.-H.; Nakashima, N.; Yamanaka, T.; Yanagida, S. *J. Phys. Chem.* **1996**, *100*, 10201.

Table 1. Crystallographic Data of **1**, **4**·CH₂Cl₂·H₂O, and **8**

	1	4 ·CH ₂ Cl ₂ ·H ₂ O	8
empirical formula	C ₆₀ H ₄₄ N ₄ P ₂ Pt	C ₉₁ H ₅₄ Cl ₂ F ₃₆ N ₄ O ₁₃ P ₂ PtYb ₂	C ₄₅ H ₂₅ F ₁₈ N ₂ O ₆ PPt _{0.5} Yb
fw	1078.02	2769.39	1333.23
space group	P $\bar{1}$	P2 ₁ /n	P2 ₁ /n
a, Å	11.1503(2)	20.594(12)	11.779(4)
b, Å	15.0906(1)	18.854(10)	27.718(9)
c, Å	15.5381(3)	27.594(17)	15.891(5)
α, deg	74.182(6)		
β, deg	83.504(7)	92.108(5)	94.628(4)
γ, deg	72.694(4)		
V, Å ³	2400.17(7)	10707(11)	5171(3)
Z	2	4	4
ρ _{calc} , g/cm ⁻³	1.492	1.718	1.712
μ, mm ⁻¹	3.034	3.236	3.295
radiation (λ), Å	0.71073	0.71073	0.71073
temp, K	293(2)	293(2)	293(2)
R1(F _o) ^a	0.0344	0.0679	0.0653
wR2(F _o ²) ^b	0.0741	0.1811	0.1105
GOF	1.041	1.079	1.149

$$^a R1 = \sum |F_o - F_c| / \sum F_o, \quad ^b wR2 = \sum [w(F_o^2 - F_c^2)^2] / \sum [w(F_o^2)]^{1/2}.$$

m/z (%) 1079 (100) ([M + H]⁺), 898 (16) ([M - bpyC≡C]⁺), 816 (10) ([M - PPh₃ + H]⁺), 719 (30) ([M - 2bpyC≡C + H]⁺). IR (KBr, cm⁻¹): 2109s (C≡C). ¹H NMR (CDCl₃, ppm): 8.61 (s, 2H, bpyC≡C), 8.22 (d, 2H, J = 7.05 Hz, bpyC≡C), 7.94 (d, 2H, J = 7.56 Hz, bpyC≡C), 7.81 (d, 14H, J = 5.82 Hz, bpyC≡C and C₆H₅), 7.72 (d, 2H, J = 7.6 Hz, bpyC≡C), 7.66 (s, 2H, bpyC≡C), 7.40 (d, 18H, J = 7.38 Hz, C₆H₅ and bpyC≡C), 6.62 (d, 2H, J = 8.07 Hz, bpyC≡C). ³¹P NMR (CDCl₃, ppm): 18.1 (t, J_{Pt-P} = 2606 Hz).

trans-Pt(PPh₃)₂(C≡Cbpy)Ln(hfac)₃)₂ (Ln = Nd, Eu, Yb). These *trans*-PtLn₂ complexes were prepared by the same synthetic procedure as that of *cis*-PtLn₂ except using *trans*-Pt(PPh₃)₂-(C≡Cbpy) (**5**) instead of *cis*-Pt(PPh₃)₂(C≡Cbpy) (**1**). Yield: 62–78%.

6 (Ln = Nd). Anal. Calcd for C₉₀H₅₀Nd₂F₃₆N₄O₁₂P₂Pt: C, 41.44; H, 1.93; N, 2.15. Found: C, 41.34; H, 2.15; N, 2.01. IR (KBr, cm⁻¹): 2111m (C≡C), 1654s (C=O).

7 (Ln = Eu). Anal. Calcd for C₉₀H₅₀Eu₂F₃₆N₄O₁₂P₂Pt: C, 41.19; H, 1.92; N, 2.13. Found: C, 41.64; H, 1.95; N, 2.21. IR (KBr, cm⁻¹): 2108m (C≡C), 1651s (C=O).

8 (Ln = Yb). Anal. Calcd for C₉₀H₅₀Yb₂F₃₆N₄O₁₂P₂Pt: C, 40.54; H, 1.89; N, 2.10. Found: C, 40.54. H, 1.81; N, 2.07. IR (KBr, cm⁻¹): 2110m (C≡C), 1654s (C=O).

Physical Measurements. Elemental analyses (C, H, N) were carried out on a Perkin-Elmer model 240C elemental analyzer. Electrospray ion mass spectra (ESI-MS) were performed on a Finnigan LCQ mass spectrometer using dichloromethane–methanol mixture as mobile phases. UV–vis absorption spectra were measured on a Perkin-Elmer Lambda 25 UV–vis spectrophotometer. Infrared (IR) spectra were recorded on a Magna750 FT-IR spectrophotometer with a KBr pellet. Emission and excitation spectra in the UV–vis region were recorded on a Perkin-Elmer LS 55 luminescence spectrometer with a red-sensitive photomultiplier type R928. Emission lifetimes in solid states and degassed solutions were determined on an Edinburgh Analytical Instrument (F900 fluorescence spectrometer) using a LED laser at 397 nm excitation, and the resulting emission was detected by a thermoelectrically cooled Hamamatsu R3809 photomultiplier tube. The instrument response function at the excitation wavelength was deconvolved from the luminescence decay. Near-infrared (NIR) emission spectra were measured on an Edinburgh FLS920 fluorescence spectrometer equipped with a Hamamatsu R5509-72 supercooled photomultiplier tube at 193 K and a TM300 emission monochromator with NIR grating blazed at 1000 nm. The NIR emission spectra were corrected via a calibration curve supplied with the instrument. The emission quantum yields (Φ) of **1**, **3**, **5**, and **7** in degassed dichloromethane solutions at room temperature

were calculated by $\Phi_s = \Phi_r(B_r/B_s)(n_s/n_r)^2(D_s/D_r)$ using [Ru(bpy)₃](PF₆)₂ in acetonitrile as the standard (Φ_{em} = 0.062), where the subscripts r and s denote reference standard and the sample solutions, respectively, and *n*, *D*, and Φ are the refractive index of the solvents, the integrated intensity, and the luminescence quantum yield, respectively.³⁹ The quantity *B* is calculated by $B = 1 - 10^{-AL}$, where *A* is the absorbance at the excitation wavelength and *L* is the optical path length. All the solutions used for determination of emission lifetimes and quantum yields were prepared under vacuum in a 10 cm³ round-bottom flask equipped with a sidearm 1 cm fluorescence cuvette and sealed from the atmosphere by a quick-release Teflon stopper. Solutions used for luminescence determination were prepared after rigorous removal of oxygen by three successive freeze–pump–thaw cycles.

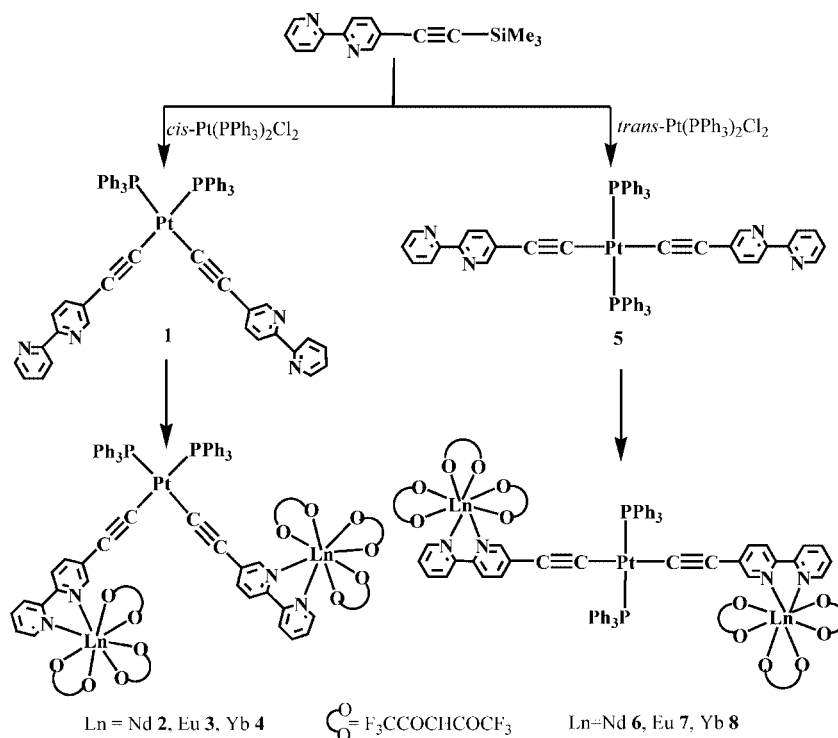
Crystal Structural Determination. Single crystals of **1**, **4**·CH₂Cl₂·H₂O, and **8** suitable for X-ray diffraction were grown by layering *n*-hexane onto the corresponding dichloromethane solutions. Crystals coated with epoxy resin or sealed in capillaries with mother liquors were measured on a SIEMENS SMART CCD diffractometer by the ω scan technique at room temperature using graphite-monochromated Mo Kα radiation (λ = 0.71073 Å). *Lp* corrections were carried out in the reflection reduction process. The structures were solved by direct methods, and the heavy atoms were located from an E-map. The remaining non-hydrogen atoms were determined from the successive difference Fourier syntheses. The non-hydrogen atoms were refined anisotropically except for the F atoms in **4** and **8**, and the hydrogen atoms were generated geometrically with isotropic thermal parameters. The structures were refined on *F*² by full-matrix least-squares methods using the SHELXTL-97 program package.⁴⁰ For **4** and **8**, the refinements were carried out by fixing the C–F distances (1.32 ± 0.01 Å) with the occupancy factors of F1–F36 and F1'–F36' being 0.50, respectively. Crystallographic data of **1**, **4**·CH₂Cl₂·H₂O, and **8** are summarized in Table 1.

Results and Discussion

Syntheses and Characterization. Synthetic routes to **1–8** are summarized in Scheme 1. The *cis*- (**1**) and *trans*-arranged (**5**) mononuclear platinum(II) bis(σ-acetylide) complexes Pt(PPh₃)₂(C≡Cbpy)₂ were synthesized by reaction of 2.3 equiv

(39) (a) Caspar, J. V.; Meyer, T. J. *J. Am. Chem. Soc.* **1983**, *105*, 5583. (b) Demas, J. N.; Crosby, G. A. *J. Phys. Chem.* **1971**, *75*, 991. (c) Chan, S. C.; Chan, M. C. W.; Wang, Y.; Che, C. M.; Cheung, K. K.; Zhu, N. *Chem.–Eur. J.* **2001**, *7*, 4180.

(40) Sheldrick, G. M. *SHELXS-97 and SHELXL-97*; University of Göttingen: Germany, 1997.

Scheme 1. Synthetic Routes to the PtLn₂ Heterotrinnuclear Complexes 1–8

of $\text{bpyC}\equiv\text{CSiMe}_3$ with $\text{cis-Pt}(\text{PPh}_3)_2\text{Cl}_2$ and $\text{trans-Pt}(\text{PPh}_3)_2\text{Cl}_2$, respectively, catalyzed by cuprous iodide via fluoride-promoted desilylation in the presence of potassium fluoride. Both the *cis* and *trans* isomers were isolated as pale yellow products, which were purified by silica gel column chromatography using dichloromethane–methanol ($v/v = 100:2$) and dichloromethane as the eluents, respectively. The *cis*- or *trans*-oriented PtLn_2 heterotrinnuclear arrays were prepared by reactions of the corresponding *cis*- or *trans*- $\text{Pt}(\text{PPh}_3)_2(\text{C}\equiv\text{Cbpy})_2$ with 2.2 equiv of $\text{Ln}(\text{hfac})_3(\text{H}_2\text{O})_2$ in dichloromethane solutions, respectively. Crystallization by layering *n*-hexane onto the corresponding dichloromethane solutions afforded PtLn_2 complexes as pale yellow crystals or microcrystals. Both **1** (*cis*) and **5** (*trans*) are insoluble in common solvents and sparingly soluble in dichloromethane and chloroform, but the latter (*trans*) is more soluble than the former (*cis*). Upon formation of the PtLn_2 complexes, however, the *cis*- PtLn_2 species is much more soluble in dichloromethane and chloroform than the corresponding *trans* isomers. It is noteworthy that the solubility of both *cis*- and *trans*- PtLn_2 complexes improves significantly compared with that of the corresponding precursor complexes **1** (*cis*) and **5** (*trans*). As revealed by X-ray crystallography and ^{31}P NMR spectral characterization (vide infra), both *cis* and *trans* isomers are kinetically stable in solutions without thermal- or light-induced isomerization during the reactions and spectroscopic measurements. This favors exact positioning of the prefabricated modules into the desired *cis*- and *trans*- PtLn_2 arrays.

1–8 were characterized by elemental analysis (C, H, and N), ESI-MS spectrometry, IR, ^1H and ^{31}P NMR spectroscopy, and X-ray crystallography for **1**, **4**, and **8**. The microanalyses indicated that the measured C, H, and N contents coincide well with the calculated values. In the IR spectra of mononuclear platinum(II) bis(σ -acetylide) complexes, a strong $\nu(\text{C}\equiv\text{C})$ frequency is observed at 2115 cm^{-1} for **1** (*cis*) and 2109 cm^{-1} for **5** (*trans*). Upon formation of PtLn_2 arrays by incorporating $\text{Ln}(\text{hfac})_3$ moieties, vibrational frequency due to the acetylide occurs at ca. 2120 cm^{-1} for *cis*- PtLn_2 complexes and ca. 2110 cm^{-1} for the corresponding *trans* isomers, together with

observation of a strong band at ca. 1650 cm^{-1} ascribed to $\nu(\text{C}=\text{O})$ vibrational frequency of $\text{Ln}(\text{hfac})_3$ units. In the ^{31}P NMR spectra of mononuclear platinum(II) bis(σ -acetylide) complexes, the *cis* complex **1** showed a set of satellite peaks centered at 21.5 ppm with $J_{\text{Pt-P}} = 1324\text{ Hz}$, whereas the corresponding signals for *trans* species **5** occurred at 18.1 ppm with $J_{\text{Pt-P}} = 1303\text{ Hz}$.

The structures of *cis*- $\text{Pt}(\text{PPh}_3)_2(\text{C}\equiv\text{Cbpy})_2$ complex **1**, *cis*- PtYb_2 species **4**, and its *trans* isomer **8** were determined by single-crystal X-ray diffraction. Selected atomic distances and angles for **1**, **4**, and **8** are presented in Table 1. ORTEP drawings of **1**, **4**, and **8** are depicted in Figures 1, 2, and 3, respectively. **1**, **4**, and **8** are all characteristic of platinum(II) square-planar structures composed of C_2P_2 donors from σ -bonded bis(acetylide) and two P donors from PPh_3 . The Pt–P and Pt–C distances are comparable to those of previously described $\text{Pt}(\text{PPh}_3)_2(\text{C}\equiv\text{CR})_2$ (R = alkyl or aryl) complexes, and the C–C lengths of acetylides are in the range $1.17\text{--}1.21\text{ \AA}$,^{28–34} suggesting a typical character of a C≡C bond. The Pt–acetylide σ -coordination is quasi-linear, as indicated by the angles of C2–C1–Pt = $171.7(3)^\circ$ and C22–C21–Pt = $179.3(4)^\circ$ for **1**,

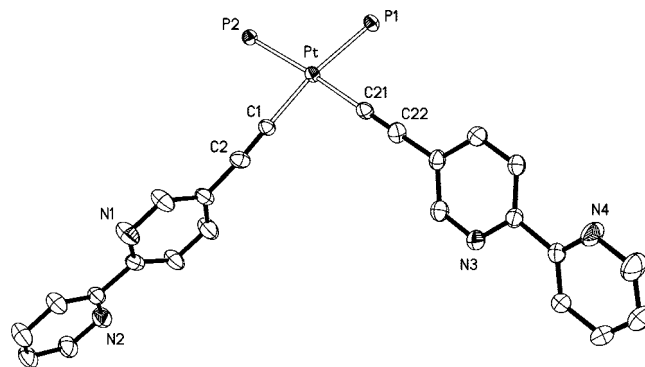


Figure 1. ORTEP drawing of **1** with atom-labeling scheme showing 30% thermal ellipsoids. Phenyl rings on the phosphorus atoms are omitted for clarity.

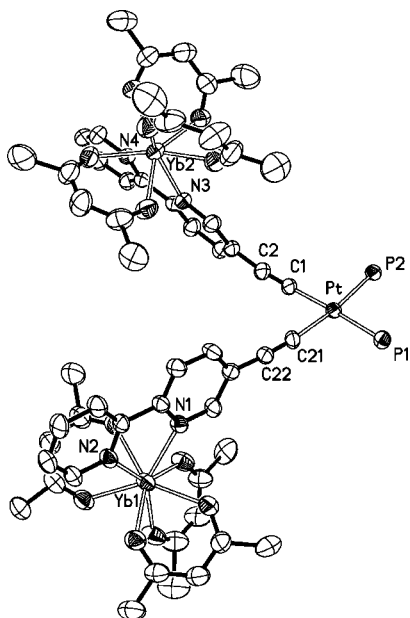


Figure 2. ORTEP drawing of **4** with atom-labeling scheme showing 30% thermal ellipsoids. Phenyl rings on the phosphorus atoms and the F atoms on the trifluoromethyl are omitted for clarity.

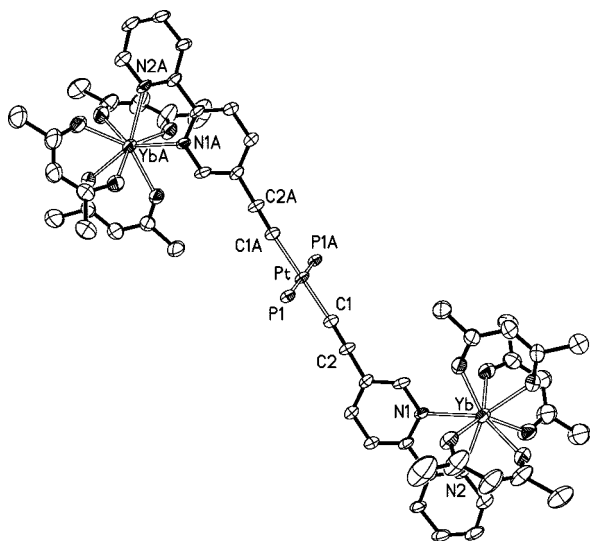


Figure 3. ORTEP drawing of **8** with atom-labeling scheme showing 30% thermal ellipsoids. Phenyl rings on the phosphorus atoms and the F atoms on the trifluoromethyl are omitted for clarity.

$C2-C1-Pt = 174.6(9)^\circ$ and $C22-C21-Pt = 175.1(8)^\circ$ for **4**, and $C2-C1-Pt = 175.4(8)^\circ$ for **8**.

For **1**, 2,2'-bipyridyl-5-acetylide is bound to the platinum(II) center through Pt-acetylide bonding, whereas the 2,2'-bipyridyl lacks coordination. Two *cis*-arranged C≡Cbp_y ligands are oriented to form a dihedral angle of 79.4° in **1**. Upon formation of *cis*-PtYb₂ complex **4** (Figure 2), the dihedral angle formed by two C≡Cbp_y ligands becomes 81.1° as a result of incorporating Yb(hfac)₃ moieties through 2,2'-bipyridyl chelation. In contrast, two *trans*-arranged C≡Cbp_y ligands in *trans*-PtYb₂ complex **8** (Figure 3) are coplanar. Because of steric requirements, the two Yb(hfac)₃ units in both **4** (*cis*) and **8** (*trans*) are oriented in opposite directions. The Yb^{III} centers are eight-coordinated with N₂O₆ donors to form a distorted square antiprism in both **4** and **8**. The Pt⋯Yb separations through bridging 2,2'-bipyridyl-5-acetylides are 8.17 and 8.67 Å in **4** and 8.47 Å in **8**. The Yb⋯Yb distance, however, is much

Table 2. Selected Interatomic Distances (Å) and Bond Angles (deg) for **1**, **4**·CH₂Cl₂·H₂O, and **8**

	1	4 ·CH ₂ Cl ₂ ·H ₂ O	8
Pt—C1	2.002 (3)	1.982 (10)	1.993 (8)
Pt—C21	2.020 (4)	2.003 (8)	
Pt—P1	2.3279 (9)	2.327 (3)	2.305 (2)
Pt—P2	2.3143 (9)	2.311 (2)	
Yb1—N1		2.465 (7)	2.459 (7)
Yb1—O1		2.292 (8)	2.304 (7)
C1—C2	1.182 (5)	1.179 (13)	1.207 (10)
C21—C22	1.179 (5)	1.196 (12)	
C2—C1—Pt	171.7 (3)	174.6 (9)	175.4 (8)
C22—C21—Pt	179.3 (4)	175.1 (8)	
C1—Pt—C21	88.80 (14)	85.3 (3)	
C1—Pt—P1	170.94 (10)	171.5 (2)	90.5 (2)
C1—Pt—P2	86.65 (10)	87.9 (2)	
C21—Pt—P1	86.14 (10)	87.6 (3)	
C21—Pt—P2	174.46 (10)	172.9 (3)	
P1—Pt—P2	98.78 (3)	99.03 (9)	
O1—Yb1—O2		73.1 (3)	72.4 (3)
O1—Yb1—N1		72.7 (3)	115.5 (3)

shorter in *cis*-PtYb₂ complex **4** (11.29 Å) than that in *trans*-isomer **8** (16.94 Å). For **4** (*cis*-PtYb₂) and **8** (*trans*-PtYb₂), the 2,2'-bipyridyls in neighboring molecules exhibit parallel arrangements with bpy⋯bpy distances in the range 3.4–3.6 Å (Figures S1 and S2, Supporting Information). This implies that intermolecular $\pi\cdots\pi$ stacking is likely operative between the 2,2'-bipyridyls in **4** and **8**.

UV–Vis Absorption Properties. UV–vis absorption and luminescence data of **1–8** are summarized in Table 2. The electronic absorption spectra of **1** and **5** (Figure S3, Supporting Information) in dichloromethane solutions display intense absorption bands at ca. 308 nm and strong broad bands at ca. 370 nm. The former with high energy is most likely ligand-centered absorptions, whereas the latter with low energy arises from metal-perturbed $\pi\rightarrow\pi^*$ (C≡C) transitions in C≡Cbp_y, mixed probably with some d(Pt)→ π^* (C≡Cbp_y) MLCT character.^{23,41,42}

Upon formation of the PtLn₂ arrays by combining **1** or **5** with Ln(hfac)₃ units through 2,2'-bipyridyl chelation, apart from occurrence of a new intense absorption at ca. 295 nm from the Ln(hfac)₃ moiety, the low-energy absorption bands due to metal-perturbed $\pi\rightarrow\pi^*$ (C≡C) and/or MLCT transitions are red-shifted ca. 30 nm to lower energy (Figures S4 and S5, Supporting Information). The 2,2'-bipyridyl chelating to Ln(hfac)₃ would lower the π^* orbital energy in the C≡Cbp_y and reduce the energy gap between HOMO (d) and LUMO (π^*), thus inducing an obvious red-shift of the metal-perturbed $\pi\rightarrow\pi^*$ (C≡C) and/or MLCT absorption. As shown in Figure 4, titration of **1** or **5** (Figure S6, Supporting Information) with Yb(hfac)₃(H₂O)₂ in dichloromethane induced the MLCT maximum shifts from ca. 370 to 400 nm when 2 equiv of Yb(hfac)₃(H₂O)₂ was added.

Luminescence Properties. Upon irradiation at 320 nm < λ_{ex} < 420 nm, **1** and **5** emit low-energy luminescence at 490–560 nm in both solid state (Figure S7, Supporting Information) and dichloromethane solutions (Figure 5) with the lifetimes in the microsecond range at 298 K, indicating a triplet state parentage. As indicated in Figure 5, a high-energy fluorescent emission also occurs at ca. 440 nm in the dichloromethane solutions of **1** or **5** with the lifetime < 10 ns at 298 K, originating most likely from an intraligand singlet excited

(41) Li, Q.-S.; Xu, F.-B.; Cui, D.-J.; Yu, K.; Zeng, X.-S.; Leng, X.-B.; Song, H.-B.; Zhang, Z.-Z. *Dalton Trans.* **2003**, 1551.

(42) Saha, R.; Qaium, M. A.; Debnath, D.; Younus, M.; Chawdhury, N.; Sultana, N.; Kociok-Kohn, G.; Ooi, L.; Raithby, P. R.; Kijima, M. *Dalton Trans.* **2005**, 2760.

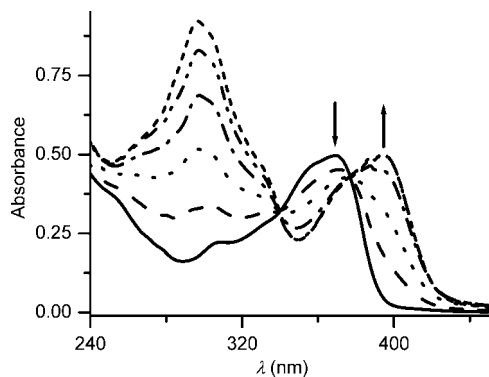


Figure 4. Titration of **1** with $\text{Yb}(\text{hfac})_3(\text{H}_2\text{O})_2$ in aerated dichloromethane solution, showing a red shift of the MLCT absorption band from the Pt^{II} acetylide chromophore.

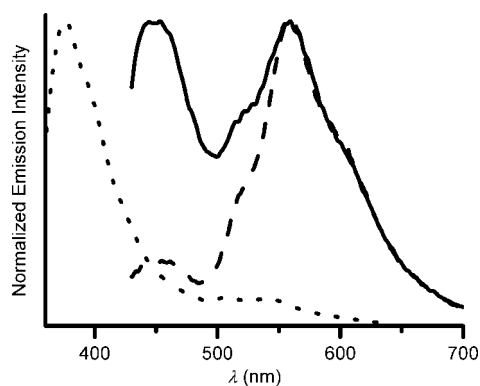


Figure 5. Emission spectra of **1** (dashes), **5** (solid line), and $\text{bpyC}\equiv\text{CSiMe}_3$ (dots) in degassed dichloromethane at 298 K.

state in 5-ethynyl-2,2'-bipyridine. Vibronic-structured emission bands with vibrational progressional spacings of 1200–1400 cm^{-1} are observed, which is typical for the $\nu(\text{C}\equiv\text{C})$ and $\nu(\text{C}\equiv\text{N})$ aromatic vibrational modes for the 2,2'-bipyridyl alkynyl ligands. The appearance of vibronic progressions suggests the involvement of the 2,2'-bipyridyl alkynyl ligand in the excited states. The room-temperature phosphorescence of **1** and **5** is thus ascribed to the extended and conjugated chromophore of the 2,2'-bipyridyl alkynyl ligand as well as the strong spin–orbital coupling induced by Pt^{II} coordination, involved probably in some $^3\text{MLCT}$ character.^{43–45} Consequently, the low-energy emissions in both **1** and **5** originate probably from an admixture of intraligand $[\pi\rightarrow\pi^*(\text{C}\equiv\text{Cbpy})]$ $^3\text{ILCT}$ and $[\text{d}\pi(\text{Pt})\rightarrow\pi^*(\text{C}\equiv\text{Cbpy})]$ $^3\text{MLCT}$ triplet excited states.^{23,41–45} It is worthy to note that the quantum yield of the low-energy emission in *cis* complex **1** ($\Phi_{\text{em}} = 0.57\%$) is ca. 3.5 times that in *trans* complex **5** ($\Phi_{\text{em}} = 0.16\%$) in degassed dichloromethane solutions.

Upon excitation at $360 \text{ nm} < \lambda_{\text{ex}} < 450 \text{ nm}$, which is the platinum(II) bis(acetylide) chromophore-based ILCT/MLCT absorption region, both *cis*- and *trans*- PtLn_2 complexes exhibit luminescence that is characteristic of the corresponding lanthanide ions. The emissive lifetimes (Table 2) of lanthanide luminescence are in microsecond ranges in both the solid state and dichloromethane solutions at room temperature. As depicted in Figure 6 and Figure S8 (Supporting Information), three emission bands occur for PtNd_2 complexes at ca. 870, 1060,

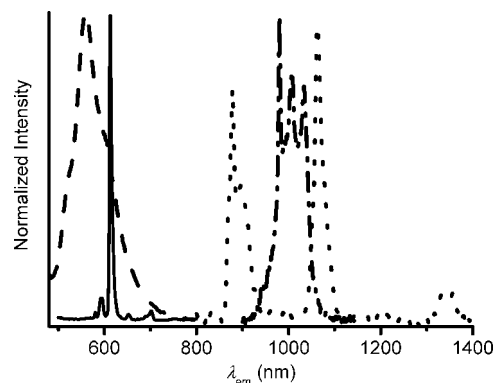


Figure 6. Emission spectra of **1** (dashes), **2** (dots), **3** (solid), and **4** (dash-dot) in dichloromethane solutions at 298 K.

and 1335 nm due to $^4\text{F}_{3/2} \rightarrow ^4\text{I}_{9/2}$, $^4\text{I}_{11/2}$, $^4\text{I}_{13/2}$ transitions, four for PtEu_2 complexes at 595, 614, 651, and 696 nm due to $^5\text{D}_0 \rightarrow ^7\text{F}_1$, $^7\text{F}_2$, $^7\text{F}_3$, and $^7\text{F}_4$, and one for PtYb_2 complexes at ca. 980 nm due to a $^2\text{F}_{5/2} \rightarrow ^2\text{F}_{7/2}$ transition. In contrast, the low-energy $^3\text{ILCT}$ and/or $^3\text{MLCT}$ emission from the Pt^{II} alkynyl chromophore in the visible region disappeared entirely, indicating that energy transfer from the Pt-based chromophore to lanthanide centers is quite complete and effective. As indicated in Table 3, lanthanide(III) luminescence including lifetimes and quantum yields in *cis*- PtLn_2 complexes is comparable to that in the corresponding *trans*- PtLn_2 isomers. Consequently, it appears that the geometrical orientation in the central platinum(II) bis(σ -acetylide) antenna chromophore exerts insignificant influence on the $\text{Pt}\rightarrow\text{Ln}$ energy transfer as well as sensitized lanthanide(III) luminescence in these *cis*- and *trans*- PtLn_2 isomeric complexes.

For both *cis*- and *trans*- PtLn_2 complexes, the high-energy fluorescence due to intraligand singlet excited states, however, is not completely quenched at 420–460 nm (Table 3). Titration of **1** or **5** with $\text{Eu}(\text{hfac})_3(\text{H}_2\text{O})_2$ (Figure S9, Supporting Information) in aerated dichloromethane induced rapid attenuation of the $\text{Pt}(\text{PPh}_3)_2(\text{acetylide})_2$ -based emission so as to complete quenching of the phosphorescence in the visible region upon addition of 2 equiv of $\text{Eu}(\text{hfac})_3(\text{H}_2\text{O})_2$. The high-energy fluorescence from the ligand-centered singlet state is partially quenched but still observed even if excess $\text{Eu}(\text{hfac})_3(\text{H}_2\text{O})_2$ is added to **1** or **5**, suggesting lower efficiency in transferring singlet state energy to the lanthanide centers, as found in a series of *cis*- PtLn_2 and Pt_2Ln_4 complexes containing the extended $\text{Pt}(\text{P}-\text{P})(\text{C}\equiv\text{CPhtpy})_2$ antenna chromophores ($\text{P}-\text{P} = \eta^2$ -chelating diphosphine, $\text{HC}\equiv\text{CPhtpy} = 4'-(4\text{-ethynylphenyl})-2,2':6',2''\text{-terpyridine}$).^{22,23}

Conclusions

cis- and *trans*- $\text{Pt}(\text{PPh}_3)_2(\text{C}\equiv\text{Cbpy})_2$ were prepared by reaction of *cis*- and *trans*- $\text{Pt}(\text{PPh}_3)_2\text{Cl}_2$ with $\text{bpyC}\equiv\text{CSiMe}_3$, respectively. Combining *cis*- or *trans*- $\text{Pt}(\text{PPh}_3)_2(\text{C}\equiv\text{Cbpy})_2$ with $\text{Ln}(\text{hfac})_3$ induced isolation of the corresponding *cis*- or *trans*- PtLn_2 isomeric complexes. These *cis*- and *trans*-oriented isomers are kinetically stable to resist thermal and photoinduced isomerization. Both *cis*- and *trans*- $\text{Pt}(\text{PPh}_3)_2(\text{C}\equiv\text{Cbpy})_2$ exhibit low-energy phosphorescence from $[\pi\rightarrow\pi^*(\text{C}\equiv\text{Cbpy})]$ $^3\text{ILCT}$ and $[\text{d}\pi(\text{Pt})\rightarrow\pi^*(\text{C}\equiv\text{Cbpy})]$ $^3\text{MLCT}$ triplet excited states together with high-energy fluorescence from a ligand-centered singlet state. Upon irradiation of *cis*- or *trans*- PtLn_2 complexes at the absorption region of a Pt-based chromophore, sensitized lanthanide luminescence is successfully attained by effective

(43) Rogers, J. E.; Cooper, T. M.; Fleitz, P. A.; Glass, D. J.; McLean, D. G. *J. Phys. Chem. A* **2002**, *106*, 10108.

(44) Haskins-Glusac, K.; Ghiviriga, I.; Abboud, K. A.; Schanze, K. S. *J. Phys. Chem. B* **2004**, *108*, 4969.

Table 3. Absorption and Emission Data of 1–8 at 298 K

compound	medium	$\lambda_{\text{abs}}/\text{nm}$ ($\epsilon/\text{M}^{-1} \text{cm}^{-1}$)	$\lambda_{\text{em}}/\text{nm}$ ($\tau_{\text{em}}/\mu\text{s}$) ^a at 298 K	$\Phi_{\text{em}} \times 10^{2b,c}$
1	solid		522 (3.3) 561 (sh)	
	CH ₂ Cl ₂	229(54 940), 308(23 700), 369(51 300)	454 (<0.01) 560 (0.1)	3.8 0.57
2	solid		460 (<0.01) 1061 (weak)	
	CH ₂ Cl ₂	228(49 270), 297(69 600), 371(41 290)	423 (<0.01) 1061 (weak)	
3	solid		440 (<0.01) 613 (69.5)	
	CH ₂ Cl ₂	228 (48 390), 303(59 770), 375(36 600)	420 (<0.01) 613 (109.5)	1.4
4	solid		462 (<0.01) 980 (13.6)	
	CH ₂ Cl ₂	228 (47 990), 297 (68 300), 371(40 500)	428 (<0.01) 980 (12.6)	0.63
5	solid		454 (<0.01) 518(1.6)	
	CH ₂ Cl ₂	229(71 900), 308(34 240), 370(78 770)	450 (<0.01) 558 (0.7)	4.3 0.16
6	solid		444 (<0.01) 1060 (weak)	
	CH ₂ Cl ₂	229(68 860), 305(61 140), 372(62 100)	421 (<0.01) 1060 (weak)	
7	solid		440 (<0.01) 613 (103.8)	
	CH ₂ Cl ₂	230(68 290), 303(60 840), 375(23 180)	415 (<0.01) 613 (216.3)	1.0
8	solid		448 (<0.01) 980 (13.8)	
	CH ₂ Cl ₂	228(48 020), 293(67 040), 384(26 870)	448 (<0.01) 980 (12.7)	0.64

^a The excitation wavelength in the lifetime measurement is 397 nm. ^b The quantum yields of **1**, **3**, **5**, and **7** in degassed dichloromethane were determined relative to that of Ru(bpy)₃(PF₆)₂ ($\Phi = 0.062$) in degassed acetonitrile. ^c The quantum yields of Yb complexes in dichloromethane solutions are estimated by the equation $\Phi_{\text{Ln}} = \tau_{\text{obs}}/\tau_0$, in which τ_{obs} is the observed emission lifetime and τ_0 is the radiative or “natural” lifetime with $\tau_0 = 2$ ms for Yb^{III}.^{5,8b,19,22} These values refer to the lanthanide-based emission process only and take no account of the efficiency of intersystem crossing and energy transfer processes.

Pt→Ln energy transfer from the Pt(PPh₃)₂(C≡Cbp_y)₂ antenna chromophore across bridging 5-ethynyl-2,2'-bipyridine with the Pt···Ln distance being 8.2–8.7 Å. While low-energy phosphorescence from the Pt-based chromophore is entirely quenched because of quite effective Pt→Ln energy transfer, high-energy fluorescence from the ligand-centered singlet state still occurs in these PtLn₂ complexes. The Pt→Ln energy transfer as well as sensitized lanthanide(III) luminescence is inappreciably influenced by the geometrical orientation of the central platinum(II) bis(σ-acetylide) antenna chromophore in these *cis*- and *trans*-PtLn₂ isomeric complexes.

Acknowledgment. This work was financially supported by the NSFC (grants 20521101, 20625101, and 20773128), the 973 project (grant 2007CB815304) from MSTC, the NSF

of Fujian Province (grants 2008I0027 and 2006F3131), and the fund from the Chinese Academy of Sciences (grant KJCX2-YW-H01).

Supporting Information Available: Figures giving additional UV–vis absorption and emission spectra, and X-ray crystallographic files in CIF format for the structure determination of compounds **1**, **4**·CH₂Cl₂·H₂O, and **8**. This material is available free of charge via the Internet at <http://pubs.acs.org>.

OM8005883

(45) Pomestchenko, I. E.; Castellano, F. N. *J. Phys. Chem. A* **2004**, *108*, 3485.